

Powder feeding enhancement of powder propellant supply system by using gas-permeable piston

Jie Tang^a, Yuxin Yang^b, Zongtao Wang^b, Haifeng Lu^{a,*}, Haifeng Liu^{a,*}

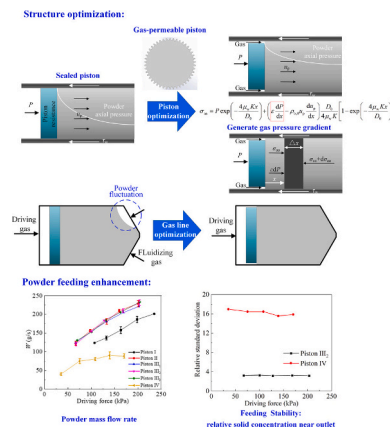
^a Shanghai Engineering Research Center of Coal Gasification, East China University of Science and Technology, Shanghai 200237, PR China

^b Science of Technology on Combustion, Internal Flow and Thermo-Structure Laboratory, Xi'an Aerospace Solid Propulsion Technology Institute, Xi'an 710072, PR China

HIGHLIGHTS

- Powder feeding enhancement by structural optimization in powder propellant supply system was realized.
- Mechanism of the use of gas-permeable piston in powder feeding was revealed.
- Influence of the structure of gas-permeable pistons on powder feeding characteristics was investigated.

GRAPHICAL ABSTRACT



ARTICLE INFO

Keywords:

Powder engine
Structural optimization
Pneumatic-driven
Feeding enhancement
Gas-permeable piston

ABSTRACT

Stable and efficient powder propellant feeding is the key to the excellent performance of powder engines, but the previous structures of supply systems pose a challenge to it. Therefore, structural optimization has been made for the powder propellant supply system to promote feeding. Specifically, the traditional sealed piston is optimized as the gas-permeable piston that has an annular gap between the piston edge and the silo wall to allow the driving gas to permeate into the powder column, producing the gas pressure gradient to increase powder axial pressure and leading to the cancellation of fluidization gas line at the front of the silo to reduce gas turbulence and powder fluctuations. There is a discovery that the powder achieves mass flow under only airflow and discharged powder amount can be maximized as much as possible by combining with gas-permeable piston, which also supports the feasibility of the optimized system and realizes a more stable and higher flux flow. In addition, the gas-permeable piston with a gear-shaped end face has the best overall performance. Through this work, we wish that our research can provide valuable guidance for the design of powder propellant supply systems to meet the requirements of spacecraft power systems.

* Corresponding authors.

E-mail addresses: luhf@ecust.edu.cn (H. Lu), hfliu@ecust.edu.cn (H. Liu).

<https://doi.org/10.1016/j.powtec.2023.118406>

Received 16 September 2022; Received in revised form 14 January 2023; Accepted 2 March 2023

Available online 7 March 2023

0032-5910/© 2023 Elsevier B.V. All rights reserved.

Nomenclature			
AOR	Angle of repose, °	R	Molar gas constant, J/(mol•K)
D_0	Silo diameter, mm	RSD	Relative standard deviation of relative solid concentration
D_1	Diameter of the end face of the piston, mm	S	Area between the piston edge and silo wall, mm ²
D_2	Diameter of the end face of the piston, mm	T	Room temperature, K
d	Outlet diameter, mm	$u_{gi, per}$	Apparent permeable gas velocity, mm/s
d_{32}	Sauter mean diameter, μm	u_p	Particle velocity, mm/s
FI	Carr flow index	V	Volume of the air cavity, m ³
H	Piston thickness, mm	W	Powder mass flow rate, g/s
K	Pressure transmission coefficient	$W_{gi, per}$	Apparent permeable gas flow rate, g/s
L_0	Initial packing powder column length in the cylinder section, mm	α	Half cone angle, °
M	Molar mass, g/mol	ε	Porosity
m_g	Mass change of the gas in the air cavity, g	μ_w	Coefficient of wall friction
$m_{g, t}$	Total mass of gas entering the silo, g	ρ_p	Particle density, kg/m ³
Δm_g	Mass of gas permeated into the powder column, g	$\rho_{b,0}$	Bulk density, kg/m ³
P	Pressure, kPa	ρ_t	Tap density, kg/m ³
q	Gas flow rate, L/min	$\rho_{g, 0}$	Density of air under standard temperature and pressure, kg/m ³
		ψ	powder utilization rate, %

1. Introduction

With the exploitation of near-earth space and the exploration of outer space by human beings, the mission of spacecraft is becoming diversified and the working environment is also more complex, which puts forward higher requirements for the power system of the spacecraft [1–3]. Researchers try to improve the conventional propulsion methods, but also actively expand the new propulsion methods. And a new type of engine using powder fuel as the propellant was proposed under this background, namely powder engine [4–6]. Due to the flexible selection and matching of powder fuel and oxidants, powder engines have been developed in various types [7–9]. And the diversified powder propellant combinations make powder engines not only applicable to space exploration but also to underwater operations and other fields, suggesting the huge application potential. Therefore, powder engines have attracted the attention of many researchers in recent years, and a series of achievements have been made in key technologies such as powder propellant feeding [10–12] and combustion [13–15].

As the core component of the powder engine, the powder propellant supply system not only requires excellent feeding performance but also considers integration and lightweight. Therefore, its design has always been a difficult challenge in the development of powder engines. Since powder fuel is a solid discrete phase composed of a large number of single particles, its own flowability is poorer than that of liquid. To achieve efficient powder transportation, Fricke et al. [16] first proposed the use of gas as the flowing carrier of powder propellant. This idea was used for reference by many researchers later, and different types of powder propellant supply systems have been designed based on this with a common point that the position of fluidizing gas line is set at the front of the silo (conical or flat bottom). Additionally, the flight attitude of the spacecraft during the working is changeable, and the powder propellant also mostly flows in the non-gravity direction, especially in the horizontal direction. Therefore, it is common practice to add a piston at the tail end of the silo to push the powder forward. And the main principle of powder feeding is that the pressure difference is created at both ends of the piston, so that the powder can be discharged from the silo in the form of gas-solid two-phase flow under the dual action of piston thrust and fluidizing gas entrainment and be sent into the combustion chamber to generate power.

Loftus et al. [17] designed a powder propellant supply system similar to the industrial fluidized bed. In addition to the fluidizing gas at the front of the silo, the gas can also enter the powder column from the piston guide rod. On this basis, Foote and Litchford [18] abandoned the

method of introducing the gas through the piston guide rod, and instead added an air collecting chamber. A portion of the gas is first collected in the collecting chamber and then enters the powder through the porous piston. Miller and Herr [8] designed a powder propellant supply system that connected the hoses to the piston, and the gas can enter the powder through the hoses, but the hoses would occupy part of the limited storage space of the silo and reduce the powder packing rate. However, the above-mentioned powder propellant supply systems all have a common point that the piston guide rod is necessary to connect with the external driving air chamber to push the piston, which makes the structure of the system more complicated and is not conducive to the integration and lightweight of the powder engine. Drawing on previous research achievements, Northwestern Polytechnical University has designed a simpler and more efficient pneumatic-driven powder propellant supply system [19,20]. The driving chamber and the fluidizing chamber in a silo are separated by a completely airtight piston without a rod. And the piston movement and powder feeding can be achieved by adjusting the flow rate of driving gas and fluidizing gas to produce sufficient pressure difference between the front and rear of the piston. Li et al. [21] verified the feasibility of the synchronization of the two-component powder supply method in this system. In addition, Sun et al. [22] conducted a detailed comparative analysis of the stability of powder choking flow using standard deviation, wavelet analysis, and higher-order statistics. However, the compressibility of the gas will cause pressure fluctuations on both sides of the piston, which may cause unstable movement of the piston and affect the powder feeding. Given the above situation, Goroshin et al. [23,24] proposed a motor-driven powder propellant supply system that connects the piston rod and the motor rod to drive the piston, and the smooth movement of the piston can be achieved by adjusting the motor rotating speed. But this puts forward a higher demand on the power of the motor. Overall, the pneumatic-driven system without the piston rod is more integrated and lighter than the motor-driven system and is also the trend of development.

However, it can be found that the pistons reported in the literature are edge-sealed or completely sealed. The friction between the piston edge and the silo wall makes the systems have higher requirements on the wear resistance of the piston and may also lead to potential problems such as large system resistance and piston stuck, which are challenges to the continuous feeding of powder. More importantly, the interaction between necessary fluidizing gas and powder at the front of the silo can result in strong gas turbulence and powder fluctuation near the outlet [12], which seriously affects the stability of powder feeding. Herein, a

pneumatic-driven powder propellant supply system using the gas-permeable piston without the fluidization gas line was designed to achieve continuous and stable high flux feeding of powder, and an emphasis on the influence of the structure of the gas-permeable piston was studied.

2. Experimental setup

2.1. Materials

Micro aluminum powder is often used as the powder propellant. However, there may be a dust explosion if micro aluminum powder disperses into the air. Considering the safety of the experiment, the neutral glass beads which have a similar flowability to the aluminum powder [25] were used as experimental materials in this work. The basic physical properties of the glass beads are shown in Table 1, and Fig. 1 presents the cumulative particle size distributions and scanning electron microscope (SEM) image of experimental materials which were obtained by using a Malvern laser particle size analyzer (Mastersizer 2000) and scanning electron microscope (HITACHI, SU-1510). The particle density (ρ_p) was measured by an automatic true density analyzer (Quantachrome 1200e). A PT-X powder tester (Hosokawa Micron Corporation) was used to obtain the bulk density (ρ_b), tap density (ρ_t), angle of repose (AOR), and Carr flow index (FI).

2.2. Apparatus and procedures

The experimental apparatus used is illustrated in Fig. 2, which is mainly composed of the aeration system and the silo. The airflow from the stable air source passes through a mass flow controller (Qixing Huachuang, CS200, the calibration condition is standard temperature and pressure) to control the gas flow rate (q) and enters the silo through a vent with an internal diameter of 10 mm of a sealed cover at the tail end of the silo. And the vent was inlaid with sintered bronze plates to avoid the particles leakage into the gas pipeline. The silo is divided into the cylinder section with an inner diameter D_0 of 50 mm and the cone section with an outlet diameter d of 5 mm and half cone angle α of 60° , which are made of transparent plexiglass. Moreover, the silo is fixed on a rotatable and grounded metal frame to eliminate electrostatic effects.

The silo was first rotated to the vertical direction before each experiment. Then, the powder was packed through a sieve into the silo to obtain the initial dense column. Let the packing powder column length $L_0 = 400$ mm in the cylinder section to keep the data comparability. Place the gas-permeable piston on the surface of the powder column and seal the end of the silo with a cover. The length of the cylinder section of the silo is the sum of the powder column length and the thickness of the piston. Finally, rotate slowly the silo to the horizontal direction to make the packing fraction unchanged and then introduce the airflow. The time series of the weight of the discharged powder were recorded by an electronic scale (the measuring range is 0–30 kg, the accuracy is 0.1 g, and the acquisition frequency is 10 Hz). The high precision flat diaphragm pressure sensors (PR-35 \times , the measuring range is 0–3000 kPa, the accuracy is 0.05%FS, and the acquisition frequency is 100 Hz) from Keller Company were used to measure the pressure signal (P), where the pressure-sensitive surface of P_2 is fixed at the wall of the cone. A high-speed camera (Photron Fastcam SA2) was used to record the discharge process and the open-source software Image J was used to process the images. The powder mass flow rate (W) is considered as the ratio of the discharged powder mass to the discharged

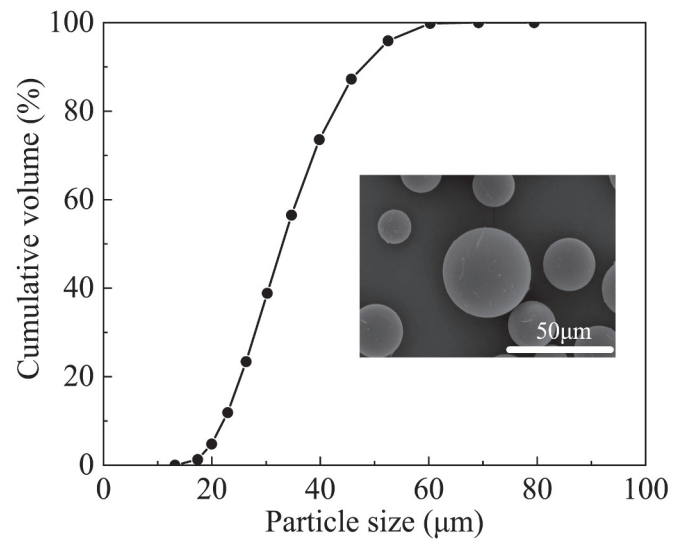


Fig. 1. Cumulative particle size distributions and SEM image of experimental materials.

time and is presented in the figures as the average value of three replicate experiments. And the ratio of the mass of discharged powder to the total mass of powder loaded as the powder utilization rate (ψ).

3. Results and discussion

3.1. Optimization of powder propellant supply system

3.1.1. Optimization of piston

According to the literature [4], the sealed piston pushes the powder in the cylinder section of the silo forward approximately as a rigid body under the action of the driving force, as shown in Fig. 3(a), which also means that the velocity of particles at the same moment is almost equal, and the inter-particle velocity gradient and shear friction can be ignored. However, the slip between the powder column and the silo wall leads to a significant speed difference and shear friction, which results in the powder axial pressure drop along the movement direction. In addition, considering the potential problems of large system resistance and easy getting stuck caused by the sealed piston, the piston optimized in this paper has a gap with the silo wall, as shown in Fig. 3(b). On the one hand, it can improve the above problems and reduce the system's requirements for piston wear resistance; on the other hand, the driving gas can penetrate into the powder column through the gap between the piston and the silo wall. Considering the microelement in Fig. 3(c), it can be obtained by force analysis:

$$\frac{d\sigma_{aa}}{dx} + \frac{4\tau_w}{D_0} = \varepsilon \frac{dP}{dx} - \rho_{b,0} u_p \frac{du_p}{dx} \quad (1)$$

Introduce the boundary condition of the powder axial pressure ($P_{aa}|_{x=0} = P$) without considering piston resistance, so the solution of Eq. (1) leads to the following equation based on Janssen theory [26–28]:

$$\sigma_{aa} = P \exp\left(-\frac{4\mu_w Kx}{D_0}\right) + \left(\varepsilon \frac{dP}{dx} - \rho_{b,0} u_p \frac{du_p}{dx}\right) \frac{D_0}{4\mu_w K} \left[1 - \exp\left(-\frac{4\mu_w Kx}{D_0}\right)\right] \quad (2)$$

Table 1
Physical parameters of experimental materials.

Material	d_{32} (μm)	ρ_p (kg/m^3)	$\rho_{b,0}$ (kg/m^3)	ρ_t (kg/m^3)	AOR ($^\circ$)	FI
Glass bead	33	2490	1370	1516	32.1	86.5

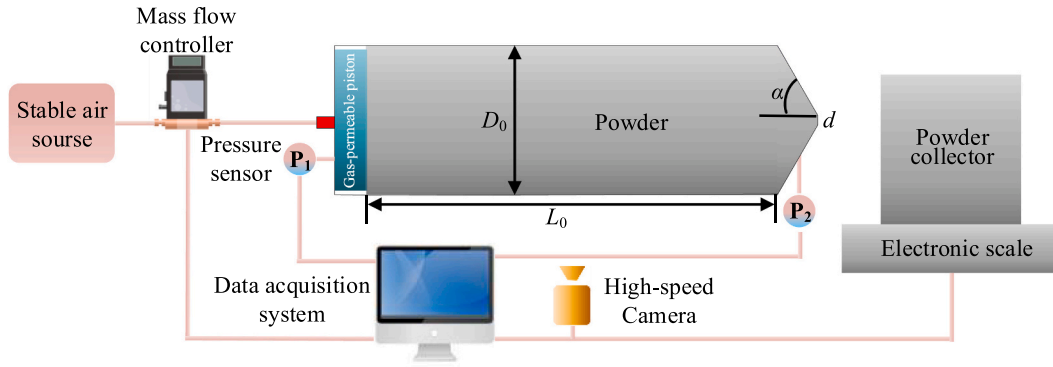


Fig. 2. Schematic illustration of the experimental system ($D_0 = 50$ mm, $d = 5$ mm, $\alpha = 60^\circ$, $L_0 = 400$ mm).

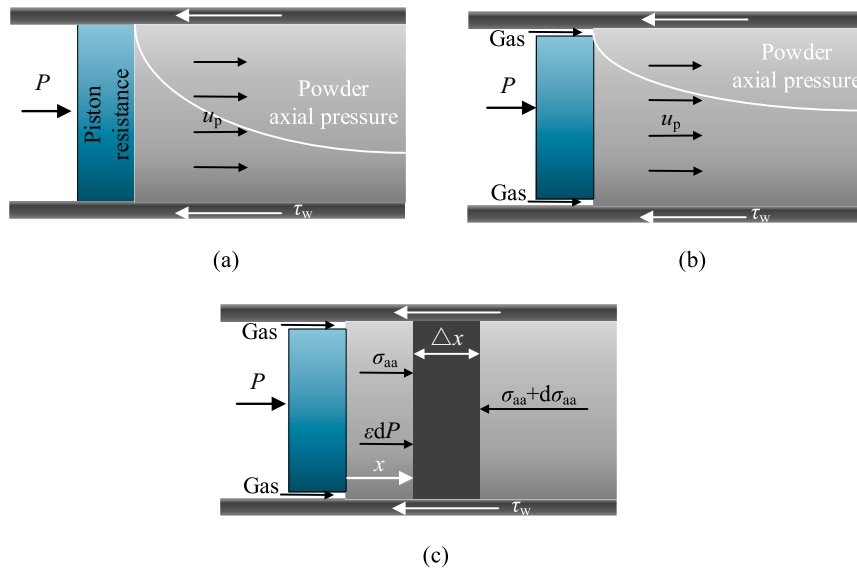


Fig. 3. (a) Schematic diagram of powder movement using sealed piston; (b) schematic diagram of powder movement using gas-permeable piston; (c) forces acting on a microelement of powder column. Optimization of the piston produces the gas pressure gradient force along the powder movement.

where μ_w is the coefficient of wall friction, and K is the stress transmission coefficient, u_p is the particle velocity. For the systems using gas-permeable piston, the flow direction of permeating gas is consistent with the powder flow, so that there is a gas pressure gradient in the powder column [29], and a pressure gradient force along the flow direction is generated on the powder to increase the powder axial pressure. And the higher axial pressure will be beneficial to the improvement of powder mass flow rate [30].

Table 2 shows the structural parameters of different pistons used in this paper. The end face of piston I is a conventional round and itself is airtight. Based on the porous piston with edge seal used in reference [18], a gas-permeable piston with the similar porous end face, namely piston II, is proposed. It also has the round end face, which is formed by connecting the porous metal plate (the thickness is 2 mm) and the hollow tube, and the gas can enter the powder column from the edge and the piston. It is worth noting that the porous metal plate used in the experiments was made by common powder compacting and sintering method, that is, copper powder with the particle size range of 177–250 μm and $d_{32} = 209$ μm was used as raw material, after compacting forming in the mold, and then heating to a temperature lower than the melting point of copper powder to bond the particles, so that the porous metal plate with a porosity of 40% was made. The sintering process changes the powder-forming billet from particle aggregate to crystal combination. Piston III has an unconventional gear-shaped end face, and

itself is also airtight like piston I, and the gas can enter the powder column from the piston edge. Piston IV which is used as a comparison has a rubber seal on the edge, and its end face is airtight. For pistons I, II, and IV, D_1 represents the diameter of the end face. For piston III, D_1 is the diameter of the addendum circle, and D_2 is the diameter of the root circle. H shows the thickness of the piston and S is the area between the piston edge and silo wall. In addition, the pressure differences required to push pistons I, II and III are all not more than 100 Pa according to the test.

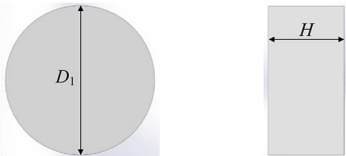
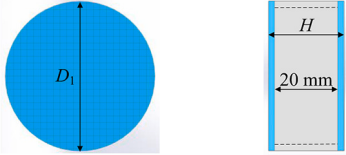
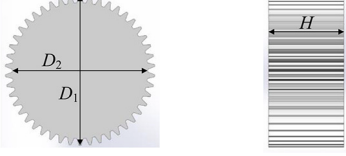


3.1.2. Optimization of gas line

Fig. 4 shows the difference in gas line between the system using sealed piston and the system using gas-permeable piston. The permeate gas can provide a similar function like the fluidizing gas at the front of the silo as the flowing carrier. In addition, considering that the fluidizing gas can cause strong gas turbulence and powder fluctuations near the outlet, the system using gas-permeable piston cancels the fluidizing gas to avoid the above problems, so that the gas line is also simplified, which is more conducive to the integration and lightweight of the powder engine.

3.2. Discharge characteristics of using different gas-permeable pistons

Fig. 5(a) shows the discharge process when piston I is used. It can be

Table 2
Structural parameters of the different pistons.

Piston		D_1 (D_2) (mm)	H (mm)	S (mm ²)	Feature
I		48	24	154	Unsealed edge; Airtight end face
II		48	24	154	Unsealed edge; Porous end face with porosity of 40%; Crystal combination
III ₁ III ₂		48 (44) 48 (44)	16 24	326 326	Unsealed edge; Airtight end face
III ₃		48 (44)	32	326	
IV		50	24	0	Sealed edge; Airtight end face

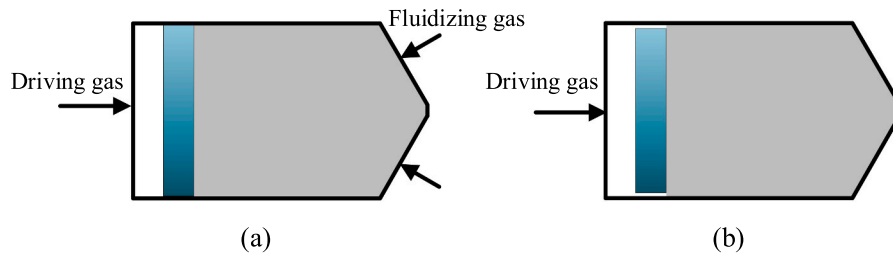


Fig. 4. Schematic diagram of powder supply system: (a) using sealed piston; (b) using gas-permeable piston.

observed that under the push of the airflow, the piston moves forward in close contact with the powder column all the time during the discharge process and the powder can be continuously discharged from the silo in the form of the mass flow. Moreover, the piston can continuously travel to the junction of the cylinder and cone of the silo at last, so that only a small part of the powder is still deposited on the cone section of the silo, which is inevitable due to gravity and gas short circuit.

Fig. 5(b) presents the discharge process when piston II is adopted. As the end face of the piston is a porous material with good air permeability, the effective pressure difference cannot be formed between the front and rear of the piston to overcome the friction between the piston and the silo wall, so the piston cannot move forward with the powder column. However, the powder column itself keeps the mass flow under the action of airflow. When the powder column is short, the mass flow ends, and the upper part of the powder column is discharged. After the airflow is connected to the atmosphere, the bottom powder spreads towards the end of the silo, leading to some powder deposited in the cylinder of the silo. Fig. 5(c) demonstrates the discharge process when piston III₂ is used. Similar to piston I, piston III₂ (also piston III₁ and III₃ without repeated displaying) can also move forward in close contact

with the powder column and travel to the junction of the cylinder and cone.

Fig. 6(a) show the time series curves of pressure (P_1) under different gas-permeable pistons. Since the gas line of the system is set at the end of the silo, the gas entering the silo will accumulate at the end of the silo due to the permeability resistance of the powder column to the gas, forming a high-pressure air cavity, which drives the piston and powder column forward. Then, the driving force is represented by the average pressure during the discharge process in this paper, as shown in Fig. 6 (b). It can be found from the results that the driving force increases with the increase of the gas flow rate. In addition, the driving force of using piston II and III₂ is close and both lower than that of using piston I.

In a word, the above experimental results confirm that the pneumatic-driven powder supply system using gas-permeable piston is a feasible method for powder feeding, such as the case of using piston I and III₂. In addition, in the knowledge of the previous systems, the powder flow during the entire discharge process all needs to be maintained by the push of the sealed piston. However, for the optimized system, there is a discovery that the powder can achieve mass flow under only the action of the airflow, such as in the case of using piston II, which

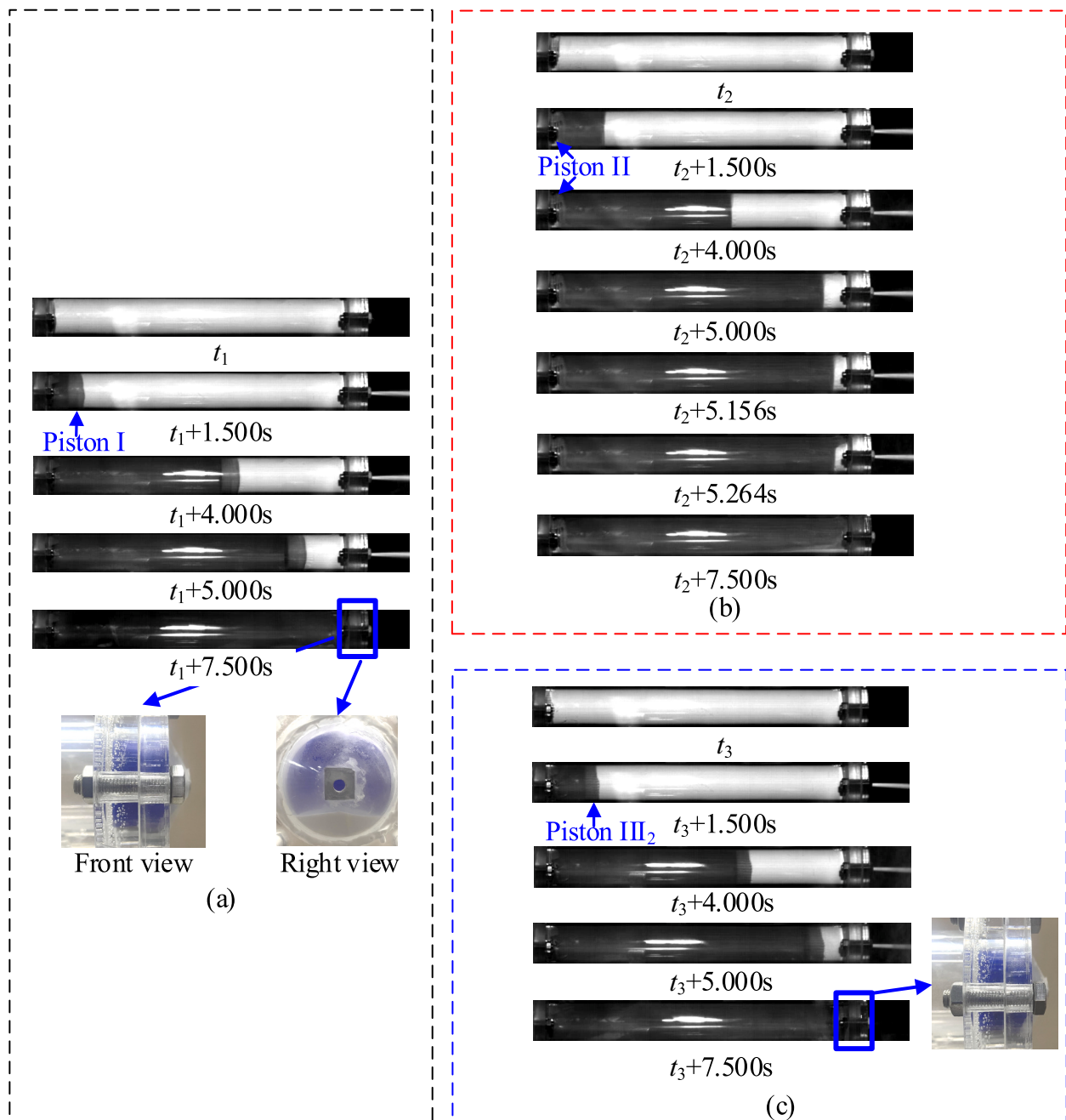


Fig. 5. Powder feeding process of using different gas-permeable pistons: (a) piston I; (b) piston II; (c) piston III₂.

is similar to the plug flow in the horizontal pipe. However, the velocity of particles in the upper layer of the plug flow is always greater than that in the lower layer [31,32]. This may lead to the problem that a lot of powder is deposited in the pipes, and a similar consideration is one of the reasons that the sealed pistons were added to supply systems reported in previous literature. But different geometries lead to different phenomena. Compared with the pipes, due to the structural constraint which the reduction of the cross-section area of the conical section of the silo, the movement of the upper layer of the powder column is hindered to become the same velocity as the lower layer to achieve the mass flow during the powder discharge. And this situation is maintained until the powder column is short. This is because the shorter powder column has less resistance to the airflow, which is not enough to balance the air pressure leading to the powder column being broken by the airflow. But this also supports the feasibility of the optimized system. Therefore, in

order to maximize the utilization of the powder, it is necessary to use the gas-permeable piston. And the role of the gas-permeable piston is slightly different from the sealed piston. On the one hand, it allows the airflow to create a gas pressure gradient along the direction of motion in the powder column. On the other hand, the pressure of the air cavity also pushes the gas-permeable piston to assist in maintaining the mass flow of the powder column and discharge the small amount of powder that should have been left in the cylinder section to improve the discharged powder mass.

3.3. Comparison of two systems

3.3.1. Powder mass flow rate

Mass flow rate is a key parameter of the powder supply system and an important indicator to measure its performance. And Fig. 7(a) compares

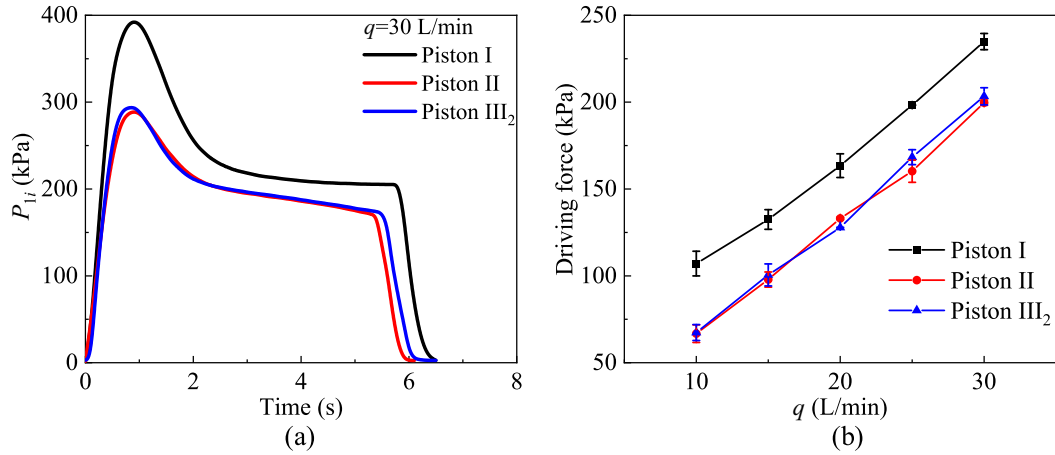


Fig. 6. (a) Pressure of air cavity over time under different gas-permeable pistons; (b) Driving force under different gas-permeable pistons. Driving force is the average pressure of air cavity over time.

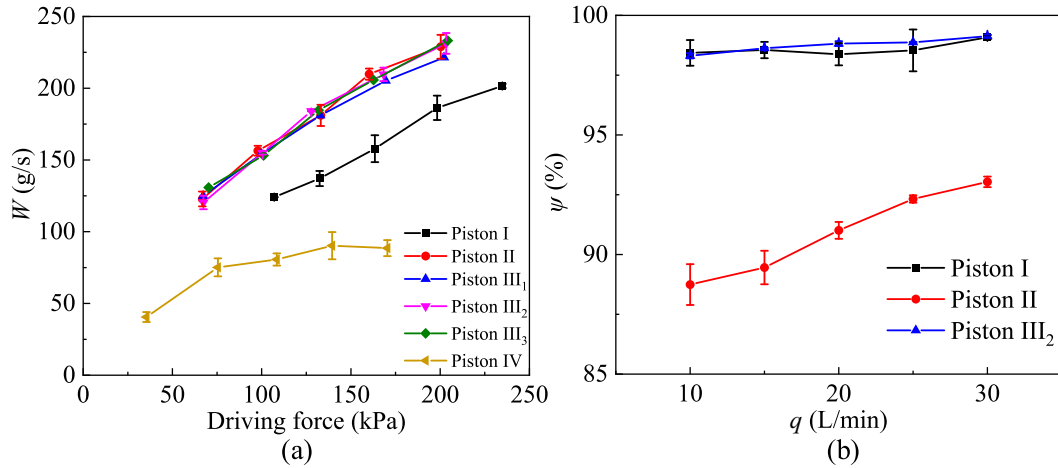


Fig. 7. (a) Relationship between powder mass flow rate and driving force under two systems; (b) powder utilization rate under different gas-permeable pistons.

the difference in powder mass flow between the system using gas-permeable piston and the system using sealed piston. It should be briefly explained that, for the latter system, the mass flow rate will first increase and then decrease with the increase of the fluidizing gas flow rate, so the maximum value is taken as the results. Then, the driving force in the figure is the result of subtracting the frictional resistance between the sealed piston and the silo wall. The results present that the powder mass flow rate increases with the increase of driving force and the system using gas-permeable piston can obtain a higher mass flow rate than that of the system using sealed piston. In addition, the powder mass flow rate of using piston II and III₂ is close and both higher than that of using piston I. However, it is particularly important that the powder can be discharged as much as possible under the premise of limited fuel packing of powder engines. And Fig. 7(b) demonstrates that

as piston I and III₂ can travel to the junction of the cylinder and cone, the powder can discharge as much as possible relative to piston II and is very close to full discharge. Further, Table 3 compares the performance of different gas-permeable pistons. As has been noted, using piston with a gear-shaped end face can not only achieve a high powder mass flow rate, but also ensure the amount of powder discharge, indicating it has the best overall performance among several types of gas-permeable pistons. And on this basis, this paper further investigates the dependence of powder mass flow rate on the piston thickness. The results in Fig. 7(a) demonstrate that the influence of piston thickness can be negligible.

As shown in the above analysis, the difference of powder mass flow rate may be related to the difference in the powder axial pressure transmitted to the outlet. Based on the ideal gas state equation, it can be known that the mass change of the gas $m_g = m_{i+1} - m_i$ in the air cavity at $t_i \sim t_{i+1}$ can be obtained by $P_1, i+1 V_{i+1} - P_1, i V_i = m_g RT/M$ for the system using gas-permeable piston, where V presents the volume of the air cavity, M is the molar mass of air, R is the molar gas constant, and T is room temperature. Then, the total mass of gas entering the system during this period is $m_{g, t} = q \rho_{g, 0} (t_{i+1} - t_i)$, where $\rho_{g, 0}$ is the density of air under standard temperature and pressure. Further, the mass of gas permeated into the powder column during this period is calculated by $\Delta m_g = m_{g, t} - m_g$.

Therefore, the apparent permeable gas flow rate $W_{gi,pre}$ at t_i can be given by $\Delta m_g / (t_{i+1} - t_i)$. At this time, the apparent permeable gas velocity

Table 3

Performance of the different gas-permeable pistons.

	Result
Piston motion characteristics	Piston I: synchronous movement with powder column Piston II: stationary while powder column is in form of mass flow Piston III: synchronous movement with powder column
Powder mass flow rate	Piston III \approx Piston II $>$ Piston I
Powder utilization rate	Piston III \approx Piston I $>$ Piston II

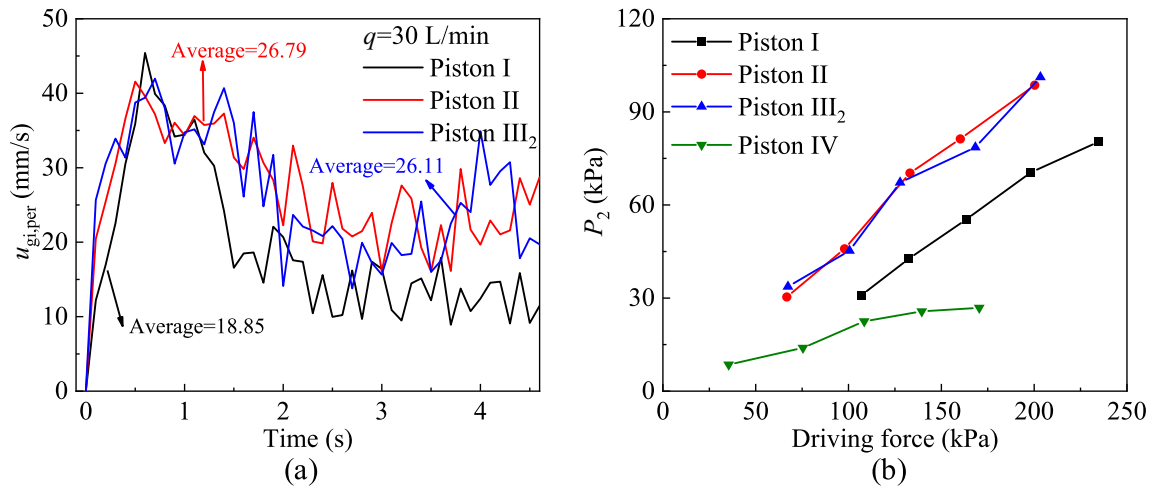


Fig. 8. (a) Apparent permeation gas velocity over time of the system using gas-permeable pistons; (b) Average pressure near the outlet of silo of two systems.

$u_{gi,per}$ is as follows $u_{gi,per} = \frac{4W_{gi,per}RT}{P_{1,i}M\pi D_0^2}$. As shown in Fig. 8(a), piston II and III₂ have larger air permeability areas compared with piston I to exist a greater apparent permeable gas velocity. And according to Ergun's equation [33], the gas pressure gradient is positively correlated with $u_{g,per}$. Therefore, there is a greater gas pressure gradient in the case of using piston II and III₂, which makes the pressure transmitted to the outlet of both greater (see Fig. 8(b)) and also indicates that the powder axial pressure near the outlet of both is greater to obtain a higher mass flow rate than the case of using piston I. However, due to the gas pressure gradient, the system using different gas-permeable pistons all achieve

higher powder axial pressures than the system using sealed piston to obtain a better flow-promoting effect.

3.3.2. Discharge stability

The presence or absence of fluidizing gas contributes to different flow patterns, which has a significant impact on the stability of powder discharge. For the system using gas-permeable piston, the powder discharges from the silo in the form of a dense gas-solid two-phase continuous jet, and this situation has never changed when the piston moves forward, as shown in Fig. 9(a). For the system using sealed piston, the fluidizing gas will collect in the upper space of the silo due to its

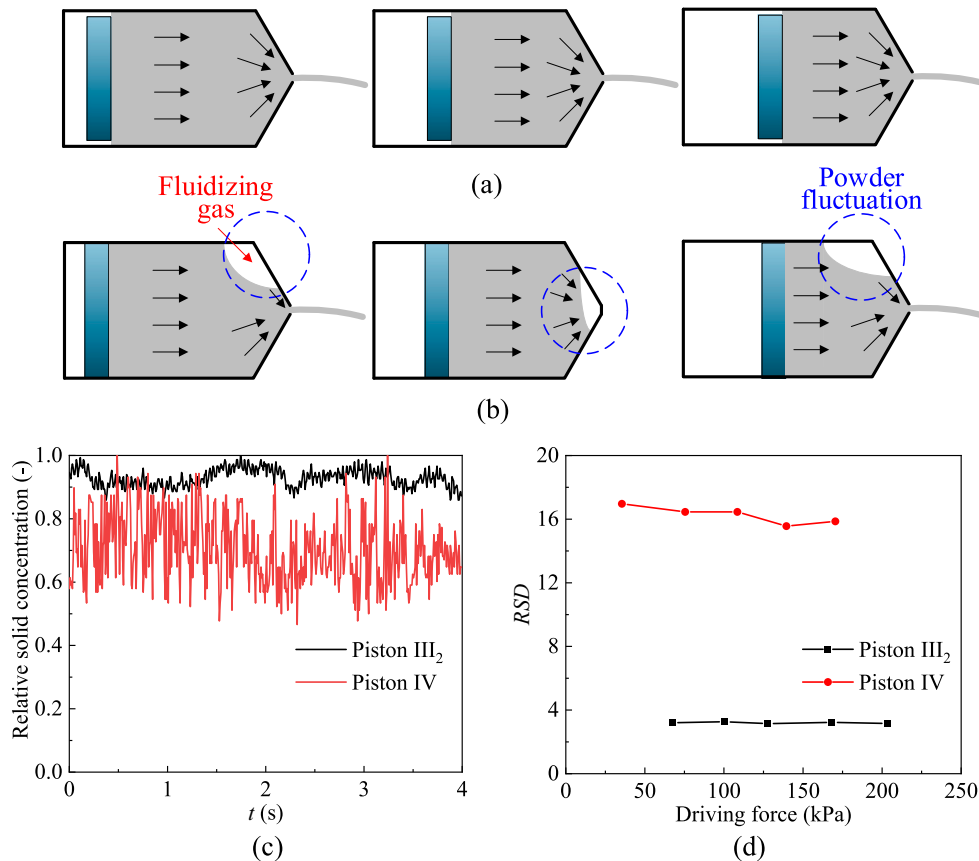


Fig. 9. (a) Schematic diagram of the discharge process of system using gas-permeable piston; (b) schematic diagram of the discharge process of system using sealed piston ; (c) relative solid concentration over time; (d) RSD of relative solid concentration during the discharge process.

density difference with the powder, creating a localized air cavity with a higher pressure than the space occupied by the powder, as shown in Fig. 9(b). This air cavity will push and entrain the powder in front of it while it also acts as a hindrance to the powder behind it. After the front powder is discharged, the air cavity is connected with the atmosphere, the pressure drops, and the behind powder is replenished near the outlet and pushed out under the action of gas pressure. This situation alternates as the piston moves forward, which leads to an intermittent jet. Fig. 9 (c)(d) shows the relative solid concentration over time of the jet at the outlet and *RSD* (relative standard deviation) of relative solid concentration during the discharge process for the two systems. The results show the relative solid concentration of the system using gas-permeable piston has a smaller fluctuation over time, which indicate that it has better discharge stability.

4. Conclusion

In summary, this paper has optimized the structure of the pneumatic-driven powder propellant supply system to enhance its feeding performance. Specifically, the sealed piston is optimized as the gas-permeable piston that has a gap between the piston edge and the silo wall to allow the driving gas to permeate into the powder column through the gap to increase powder axial pressure. Since the fluidizing gas introduced at the front of the silo will cause strong gas turbulence and powder fluctuations near the outlet, and the permeate gas can provide a similar function to the fluidizing gas as a flowing carrier, the fluidizing gas line further canceled, and only remain the driving gas line at the end of the silo, which is also more conducive to the integration and lightweight of the powder engine. The feasibility of the optimized pneumatic-driven powder propellant supply system using gas-permeable piston is verified by experiments, and a higher powder mass flow rate and better discharge stability are achieved. In addition, the influence of the structure of the gas-permeable piston on the powder feeding characteristics is studied, and the results show that the piston with the gear-phased end face has the best overall performance among several types of gas-permeable pistons based on evaluation indexes of powder mass flow rate and powder utilization rate. This brings more imagination to the feeding of powder propellants and may play a positive role in the development of powder engines.

CRedit authorship contribution statement

Jie Tang: Conceptualization, Methodology, Writing – original draft, Investigation, Writing – review & editing. **Yuxin Yang:** Visualization, Investigation. **Zongtao Wang:** Supervision. **Haifeng Lu:** Writing – review & editing, Formal analysis. **Haifeng Liu:** Validation, Project administration, Funding acquisition.

Declaration of Competing Interest

The authors declare that they have no known competing financial interests or personal relationships that could have appeared to influence the work reported in this paper.

Data availability

The authors do not have permission to share data.

Acknowledgments

The authors acknowledge the financial support from the National Natural Science Foundation of China (51876066), the Institute of Xi'an Aerospace Solid Propulsion Technology (SY41YYF2022003), and the Shanghai Engineering Research Center of Coal Gasification (18DZ2283900).

References

- [1] R.L. Ash, W.L. Dowler, G. Varsi, Feasibility of rocket propellant production on Mars, *Acta Astronaut.* 5 (1967) 705–724.
- [2] J. Linnell, T. Miller, A Preliminary Design of a Magnesium Fueled Martian Ramjet Engine, 38th AIAA/ASME/SAE/ASEE Joint Propulsion Conference & Exhibit, Indianapolis, Indiana, USA, 2002.
- [3] E.Y. Shafirovish, A.A. Shiryayev, U.I. Goldshleger, Magnesium and carbon dioxide - a rocket propellant for Mars missions, *J. Propuls. Power* 9 (1995) 197–203.
- [4] H.J. Sun, C.B. Hu, T. Zhang, Z. Deng, Experimental investigation on mass flow rate measurements and feeding characteristics of powder at high pressure, *Appl. Therm. Eng.* 102 (2016) 30–37.
- [5] R. Gordon, Powder rocket tests of the C.R.S.: initial experiments of the California Group, *Astronautics*. 11 (2015) 10–12.
- [6] J.W. Parsons, Experiments with powder motors for rocket propulsion by successive impulse, *Astronautics*. 9 (1971) 4–11.
- [7] H. Loftus, D. Marshall, L. Montanino, Powder Rocket Feasibility Evaluation, Bell Aerosystems Co., Buffalo, NY, 1973.
- [8] T. Miller, J. Herr, Green Rocket Propulsion by Reaction of Al and Mg Powders and Water, 40th AIAA/ASME/SAE/ASEE Joint Propulsion Conference and Exhibit, Fort Lauderdale, Florida, USA, 2004.
- [9] Y. Saburo, S. Kou, An examination on some technical problems of a CO₂-breathing turbojet engine in the Mars atmosphere, 36th AIAA/ASME/SAE/ASEE Joint Propulsion Conference and Exhibit, Las Vegas, NV, USA, 2000.
- [10] H.J. Sun, C.B. Hu, X.F. Zhu, J.G. Yang, Experimental investigation on incipient mass flow rate of micro aluminum powder at high pressure, *Exp. Thermal Fluid Sci.* 83 (2017) 231–238.
- [11] H.J. Sun, C.B. Hu, X.F. Zhu, Numerical simulation on the powder propellant pickup characteristics of feeding system at high pressure, *Acta Astronaut.* 139 (2017) 85–97.
- [12] H.J. Sun, C.B. Hu, Y.H. Xu, Pressure fluctuations analysis on the powder fluidization performance at different pressure, *Int. J. Multiphase Flow* 116 (2019) 176–184.
- [13] C. Li, C.B. Hu, X. Xin, Y. Li, H.J. Sun, Experimental study on the operation characteristics of aluminum powder fueled ramjet, *Acta Astronaut.* 129 (2016) 74–81.
- [14] T.R. Sippel, S.F. Son, G.A. Risha, R. Yetter, Combustion and Characterization of Nanoscale Aluminum and Ice Propellants, 44th AIAA/ASME/SAE/ASEE Joint Propulsion Conference & Exhibit, Hartford, USA, 2008.
- [15] X.F. Zhu, C. Li, Y. Guo, W. Ao, S.N. Liu, C.B. Hu, Experimental investigation on the ignition and combustion characteristics of moving micron-sized Mg particles in CO₂, *Acta Astronaut.* 167 (2020) 66–74.
- [16] H.D. Fricke, J.W. Burr, M.G. Sobieniak, Fluidized Powders-a New Approach to Storable Missile Fuels, 12th JANNAF Liquid Propulsion Meeting, 1970.
- [17] H. Loftus, L. Montanino, R. Bryndle, Powder Rocket Feasibility Evaluation, AIAA/ASEE 8th Joint Propulsion Specialist Conference, Joint Propulsion Conferences, 1972.
- [18] J.P. Foote, R.J. Litchford, Powdered Magnesium: Carbon Dioxide Combustion for Mars Propulsion, 41st AIAA/ASME/SAE/ASEE Joint Propulsion Conference, Tucson, Arizona, USA, 2005.
- [19] C. Li, X.F. Zhu, Z. Deng, J.G. Yang, C.B. Hu, J.J. Wei, Powder feeding in a powder engine under different gas-solid ratios, *Acta Astronaut.* 189 (2021) 712–721.
- [20] J.G. Yang, C.B. Hu, W. Qiang, J.M. Hu, X. Hu, X.F. Zhu, Experimental investigation on the starting and flow regulation characteristics of powder supply system for powder engines, *Acta Astronaut.* 180 (2021) 73–84.
- [21] Y. Li, C.B. Hu, Z. Deng, C. Li, H.J. Sun, Y.P. Cai, Experimental study on multiple-pulse performance characteristics of ammonium perchlorate/aluminum powder rocket motor, *Acta Astronaut.* 133 (2016) 455–466.
- [22] H.J. Sun, C.B. Hu, Y.H. Xu, Multiscale analysis of powder-propellant conveying stability through a nozzle, *J. Fluids Eng.* 140 (2019), 101302.
- [23] S. Goroshin, A.J. Higgins, J.H.S. Lee, Powdered magnesium-carbon dioxide propulsion concepts for Mars missions, 35th AIAA/ASME/SAE/ASEE Jt. Propuls. Conf. Exhib, AIAA, Los Angeles, California, USA, 1999.
- [24] S. Goroshin, A.J. Higgins, M. Kamel, Powdered metals as fuel for hypersonic ramjets, 37th AIAA/ASME/SAE/ASEE Joint Propulsion Conference and Exhibit, AIAA, Salt Lake City, Utah, USA, 2001.
- [25] J. Tang, H.F. Lu, X.L. Guo, H.F. Liu, Discharge characteristics of non-gravity-driven powder in horizontal silos, *Powder Technol.* 400 (2022), 117234.
- [26] Y. Jin, H.F. Lu, X.L. Guo, X. Gong, Characteristics and formation mechanism of plug flow in the industrial vertical pipeline of dense-phase pneumatic conveying of pulverized coal, *Chem. Eng. Sci.* 205 (2019) 319–331.
- [27] S. Shaul, H. Kalman, Friction forces of particulate plugs moving in vertical and horizontal pipes, *Powder Technol.* 256 (2014) 310–323.
- [28] M. Sperl, Experiments on corn pressure in silo cells – translation and comment of Janssen's Paper from 1895, *Granul. Matter* 8 (2005) 59–65.
- [29] Y.X. Zhou, P. Lagrée, S. Popinet, P. Ruyer, P. Aussillous, Gas-assisted discharge flow of granular media from silos, *Phys. Rev. Fluids*. 4 (2019), 124305.
- [30] M.A. Madrid, J.R. Darias, L.A. Pugnali, Forced flow of granular media: breakdown of the Beverloo scaling, *EPL*. 123 (2018) 14004.
- [31] M. Sakai, S. Koshizuka, Large-scale discrete element modeling in pneumatic conveying, *Chem. Eng. Sci.* 65 (2009) 533–539.
- [32] S. Shaul, H. Kalman, Three plugs model, *Powder Technol.* 283 (2015) 579–592.
- [33] S. Ergun, Fluid flow through packed column, *Chem. Eng. Prog.* 48 (1952) 89–94.